NASA TN D-3998

EXPERIMENTAL HEAT-TRANSFER INVESTIGATION OF NONWETTING, CONDENSING MERCURY FLOW IN HORIZONTAL, SODIUM-POTASSIUM-COOLED TUBES

By Roy A. Lottig, Richard W. Vernon, and William D. Kenney

Lewis Research Center
Cleveland, Ohio

NATIONAL AERONAUTICS AND SPACE ADMINISTRATION

For sale by the Clearinghouse for Federal Scientific and Technical Information
Springfield, Virginia 22151 – CFSTI price $3.00

EXPERIMENTAL HEAT-TRANSFER INVESTIGATION OF NONWETTING, CONDENSING MERCURY FLOW IN HORIZONTAL, SODIUM-POTASSIUM-COOLED TUBES

by Roy A. Lottig, Richard W. Vernon, and William D. Kenney

Lewis Research Center

SUMMARY

Local heat-transfer and static-pressure data were obtained for mercury condensing inside horizontal tubes cooled by sodium-potassium (NaK). Test section 1 had a constant mercury-tube inside diameter of 0.37 inch. The inside diameter of the mercury tube of test section 2 decreased from 0.46 to 0.20 inch over a length of 40 inches. The mercury flow rate was varied from 126 to 190 pounds per hour. The coolant flow rate was varied from 376 to 726 pounds per hour. The condensing length ranged from 9 to 42 inches.

The NaK film heat-transfer coefficient was evaluated from test section 1 data and varied from 2530 to 6750 Btu per hour per square foot per ^{o}F (Btu/(hr)(sq ft)(^{o}F)), which corresponds to a Nusselt number range from 3.5 to 9.3. The NaK Peclet number varied from 65 to 127. The overall condensing heat-transfer coefficient was evaluated from data obtained from test section 2. Several methods were employed to obtain the axial mercury-temperature profile required to evaluate the overall condensing heat-transfer coefficient. These methods assumed saturation temperatures for mercury-pressure profiles obtained from the measured local static pressures and for mercury-pressure profiles calculated by employing the two-phase friction-pressure-drop correlations proposed by Lockhart and Martinelli and by Koestel, Gutstein, and Wainwright (NASA Technical Note D-2514). In addition, a constant mercury temperature was assumed to determine the effect of neglecting the saturation-temperature variation on the overall condensing heat-transfer coefficient.

The values of the overall condensing heat-transfer coefficient varied with condensing length from 1650 to 3420 Btu/(hr)(sq ft)(^{o}F) for a constant axial mercury-temperature profile. Overall coefficients that were independent of condensing length were obtained for varying mercury-temperature profiles; the averages of these coefficients ranged from 2920 to 3200 Btu/(hr)(sq ft)(^{o}F). The mercury-condensing heat-transfer coefficient was concluded to be significantly larger than the NaK film heat-transfer coefficient for test section 2; therefore, the NaK film heat-transfer coefficient limited the rate of heat transfer to a greater extent than the mercury-condensing coefficient.

INTRODUCTION

Liquid-metal Rankine-cycle turbogenerator systems are currently being considered for the generation of electrical power for space applications. One example of such a system is the proposed SNAP-8 powerplant that utilizes mercury as the working fluid. A eutectic mixture of 22 percent sodium and 78 percent potassium (NaK) is employed in two separate loops as a heat source and as a coolant. In the mercury loop, thermal energy is converted into mechanical energy as mercury vapor is expanded through a turbine. The turbine exhaust enters a condenser, where thermal energy is transferred from the mercury to the NaK.

The SNAP-8 condenser is a counterflow heat exchanger with the mercury vapor condensing inside a bundle of 73 tapered-diameter tubes.

Accurate predictions of the overall condensing heat-transfer coefficient, the mercury-condensing coefficient, and the NaK film coefficient are necessary to assure compatibility of the condenser with the design requirements of the turbine and the pump components. Considerable experimental (refs. 1 to 4) and analytical work (refs. 5 to 9) has been completed to define the condensing and the film coefficients of liquid metals. Significant disagreements exist, however, between the experimental and the analytical results. In addition, little work has been done to define the magnitudes of the heat-transfer coefficients for mercury-NaK counterflow heat exchangers. In recognition of these problems, an experimental investigation was conducted to obtain data that would help define the overall condensing heat-transfer coefficient, the mercury-condensing coefficient, and the NaK film coefficient of the SNAP-8 condenser.

Single tube-and-shell test sections were chosen for this investigation to simulate the performance of a typical tube in the SNAP-8 condenser. The mercury and NaK flow-rate ranges studied were 126 to 190 pounds per hour and 376 to 726 pounds per hour, respectively. This report presents the experimental overall heat-transfer coefficients, the NaK film coefficient, and the magnitude of expected mercury-condensing coefficient obtained for single-tube heat exchangers with the nonwetting, condensing flow of mercury vapor cooled by NaK flowing countercurrently in an annulus.

EXPERIMENTAL FACILITY

The mercury and NaK loops are shown schematically in figure 1. The location and calibration range of the pressure transducers used on the test facility are shown in table I. Liquid mercury was stored in the expulsion unit, from which flow was obtained by pressurization with argon gas. After the mercury passed through an orifice, the boiling of the mercury was accomplished in three stages. The liquid mercury was first

heated to the approximate saturation temperature in the preheater. After the preheating, the liquid mercury entered a high-heat-flux unit designed to raise the vapor quality to approximately 25 percent. The mercury mixture then entered the main boiler, where electric power was applied directly to helically formed flattened tubing that formed the mercury flow passage. To minimize any liquid carryover, the mercury mixture was passed into a plenum chamber (part of the boiler), which was partly filled with stainless-steel cuttings. The mercury vapor leaving the boiler passed through a NaK-cooled desuperheater and then passed through a venturi flowmeter prior to entering the test section. Liquid mercury from the test section outlet flowed into a receiver, which in turn drained into a transfer vessel. The transfer vessel, when isolated from the receiver by a valve, was pressurized to transfer mercury back into the expulsion unit.

The NaK loop can be traced in figure 1 starting at the electromagnetic pump. From the pump, the NaK flowed through an electromagnetic flowmeter and then through a heater, which was used to control the NaK temperature in the test section. The NaK then flowed through the test section counter to the mercury flow. From the test section, a portion of the NaK went to the desuperheater while the remainder bypassed the desuperheater. The NaK inlet temperature to the desuperheater was maintained approximately 5° F above the mercury saturation temperature in the desuperheater to avoid condensing the mercury vapor. The two NaK flows then combined before entering an air cooler. A heater upstream of the air cooler was used during the NaK heating period and was turned off after mercury flow was initiated. From the air cooler, the NaK returned to the electromagnetic pump. Other branches of the NaK loop shown in figure 1 were used for filling, filtering, and draining.

SYSTEM INSTRUMENTATION

The liquid-mercury flow rate was determined by measuring the pressure drop across the calibrated orifice located at the outlet of the expulsion unit, while the vapor flow rate was determined at the venturi located upstream of the condenser inlet. The amount of NaK flow was set by the electromagnetic pump, with the flow rate being measured by an electromagnetic flowmeter. All pertinent temperatures and pressures were recorded by a central automatic digital data encoder system and by an oscillograph recorder.

DESCRIPTION OF TEST SECTIONS

Test Section 1

Test section 1 was a straight, constant-diameter tube-and-shell heat exchanger with

47 inches of heat-transfer length (fig. 2(a)). The tube in which the mercury vapor was condensed had a 0.37-inch inside diameter and a wall thickness of 0.065 inch. The shell, which formed the NaK flow annulus, had a 0.745-inch inside diameter and a 0.065-inch-thick wall. Both the tube and the shell were fabricated from 304 stainless steel.

All thermocouples used on test section 1 were constructed from Chromel-Alumel, ISA calibration K wire. Two grooves 9 and 17 inches long, 0.025 inch wide, and 0.035 inch deep were machined axially from the mercury inlet end of the tube and were 180° apart circumferentially. Three grooves 9, 17, and 25 inches long and with the same width and depth were machined in the axial direction from the mercury outlet end of the tube. These three grooves were circumferentially 120° apart. Single thermocouples were so placed in each groove that their measuring junctions were at 7.5, 15.5, 23.5, 31.5, and 39.5 inches from the mercury heat-transfer inlet. The thermocouples in the grooves were constructed from 38-gage wire and were in a 304 stainless steel sheath with a 0.02-inch outside diameter. All five thermocouples were covered by microbrazing with LM 4777.

At each of the five tube-wall-thermocouple locations, three thermocouples, circumferentially 120° apart, were inserted radially through the shell to the midpoint of the NaK annulus. At the NaK inlet and outlet, two thermocouples were inserted into the stream, while single thermocouples were spotwelded to the mercury-tube surface at the inlet and the outlet. In addition, 33 thermocouples were spotwelded to the outside surface of the shell. Starting at 4 inches from the mercury heat-transfer inlet, 10 thermocouples were spotwelded on the shell surface, one every 2 inches to 22 inches, and 23 additional thermocouples were attached at 1-inch intervals, to 45 inches from the mercury heat-transfer inlet.

The static pressures for test section 1 were measured with linear-variable-differential-transformer pressure transducers. These transducers were used to measure the inlet and the outlet static pressures of the mercury and the NaK.

Test Section 2

The mercury tube of test section 2 (fig. 2(b)) was uniformly tapered from 0.46 to 0.20 inch (nominal inside diameters) for a length of 40 inches and had a 0.035-inch-thick wall. A constant-diameter tube with the same wall thickness and approximately 12 inches long was welded to the small end of the tube. The shell with a 0.035-inch-thick wall was so tapered that a constant annular height of 0.103 inch was maintained along the axial length of the tapered portion of the test section. A straight tube section approximately 9.0 inches in length with a 0.476-inch inside diameter and a wall thick-

ness of 0.035 inch was welded to the NaK inlet end of the shell. The tube, through which the mercury flowed, was made of 9M stainless steel (9 chormium, 1 molybdenum), while the shell was fabricated from 316 stainless steel.

The thermocouples used on test section 2 were constructed from Chromel-Constantan wires. At each of five axial locations (4, 9, 14, 19, and 27 in. from the mercury heat-transfer inlet), three sheathed thermocouples, 90° apart, were inserted radially to the midpoint of the NaK annulus. At both the NaK inlet and the outlet, thermocouples were inserted into the NaK stream. On the mercury-tube surface, thermocouples were spot-welded at the inlet and the outlet. Starting at 2 inches from the mercury heat-transfer inlet, 44 thermocouples were spotwelded on the surface of the shell at 1-inch intervals in the axial direction.

The mercury static pressures on test section 2 were measured at the inlet and the outlet and at 12, 25, and 38 inches from the mercury heat-transfer inlet. The static pressures at the inlet and the outlet were measured with inductance transducers, while those at 12, 25, and 38 inches from the mercury heat-transfer inlet were measured with a resistance strain-gage transducer. All pressure transducers on test section 2 were differential instruments and were mounted horizontally with the high-pressure side connected to the test section and the low-pressure side connected to a common reference manifold.

PROCEDURE

For test section 2, prior to each data run, a complete calibration of the absolute and differential-pressure transducers was obtained. Before the pressure transducers were calibrated, the short horizontal coupling tube and the transducer cavity were filled with liquid mercury to simulate test conditions. All test-section differential-pressure transducers were calibrated simultaneously by pressurizing the mercury system with gaseous nitrogen through the venturi. All low-pressure sides were opened to atmospheric pressure, and a selected range of pressures was applied to the system. The desired oscillograph and visual readout gage spans were adjusted, and recorded runs were made over the calibration range so that transducer calibration curves could be plotted. The absolute-pressure transducers were also calibrated simultaneously by applying a known pressure to the entire system. In order to zero these transducers, the system was first pumped down to a vacuum of approximately 1 torr.

After the NaK lines were filled, power was applied to the electromagnetic pump to start the NaK circulating. The NaK flow rate was indicated by a digital readout of the voltage signal from the electromagnetic flowmeter. As the NaK was circulating, its temperature was raised to approximately 650° F. During this NaK heating period, the

mercury loop was evacuated to approximately 0.2 torr in an effort to eliminate noncondensables, and the mercury heaters were brought to operating temperatures.

With all temperatures at the desired level, the mercury preheater was turned on, and mercury flow initiated. Initially, the mercury flow rate was set at approximately 100 pounds per hour, and mercury vapor was allowed to purge the system for approximately 3 minutes in a further attempt to remove remaining noncondensables from the lines. After the purge, the mercury and NaK flow rates and the NaK inlet temperatures to the test section were set. Then the mercury receiver pressure was adjusted to locate the interface at the desired position in the test section. During loop operation, the mercury liquid-vapor interface location was obtained from the NaK shell temperature profile, which was displayed on a profile monitor.

In another series of runs, a test section similar to test section 2, but with a thinner wall, was operated. The mercury liquid-vapor interface location was determined in the thinner-wall test section by utilizing an X-ray unit and comparing it with the NaK shell temperature profile. The two methods of determining the interface location agreed within ±1 inch.

METHOD OF ANALYSIS

The experimental data used to determine heat-transfer coefficients for the single-tube heat exchangers were obtained from the test conditions presented in table II. The equations employed to determine the heat-transfer coefficients are presented subsequently. All symbols are defined in appendix A. The equations are derived in appendix B.

NaK Film Heat-Transfer Coefficient

The local NaK film heat-transfer coefficient was evaluated from test section 1 data by equation (B2):

$$h_{NaK} = \frac{1}{\frac{T_w - T_{NaK}}{\frac{Q}{A_o}} - \frac{r_o \ln\left(\frac{r_o}{r}\right)}{k_w}} \tag{B2}$$

The tube wall temperatures were obtained from measured values. The NaK stream temperatures were chosen from a curve faired through the averages of the local meas-

ured NaK stream temperatures. This curve was drawn with the NaK shell temperature profile as a guide. Temperatures from this faired curve were used to obtain the local heat flux Q/A_o at the outside surface of the tube.

Overall Condensing Heat-Transfer Coefficient

The overall condensing heat-transfer coefficient U was determined axially along the condensing length for test section 2. The coefficient was obtained by evaluating the slope of $\int U\,dA_i$ or $\int U\pi D_i\,dL$ plotted as a function of $\int dA_i$. The value of $\int U\pi D_i\,dL$ was evaluated over 1-inch increments from equation (B6):

$$\int_{L_1}^{L_2} U\pi D_i\,dL = W_{NaK}c_p\left[\ln\frac{\left(T_{Hg}-T_{NaK}\right)_{L_2}}{\left(T_{Hg}-T_{NaK}\right)_{L_1}} - \int_{L_1}^{L_2}\frac{\frac{dT_{Hg}}{dL}}{T_{Hg}-T_{NaK}}\,dL\right] \tag{B6}$$

The integral $\int dA_i$, which is equivalent to $\int \pi D_i\,dL$, was evaluated from the physical dimensions of the tube for 1-inch increments. In equation (B6), the NaK flow rate and local NaK stream temperatures were obtained experimentally, while the specific heat was determined from reference 10. The remaining parameter needed to evaluate equation (B6) is the local mercury temperature. Since the local mercury temperature was not acquired experimentally, the mercury temperature was assumed to be the local saturation temperature corresponding to the local static pressure obtained from either an assumed or a predicted static-pressure profile. The saturation temperature as a function of pressure was obtained from reference 10. Five static-pressure profiles were used independently and were determined by (1) assuming a constant pressure equal to the measured inlet static pressure; (2) connecting the measured static pressures with straight lines; (3) and (4) using the method proposed by Lockhart and Martinelli to evaluate two-phase friction-pressure losses (ref. 11) with the momentum changes calculated by assuming liquid-to-vapor velocity ratios of 0.5 and 1.0, respectively; and, finally, (5) employing the fog-flow correlation proposed by Koestel, Gutstein, and Wainwright to predict the two-phase friction-pressure losses (ref. 12) with a liquid-to-vapor velocity ratio of 1.0.

Reference 13 presents a comparison of the static pressures predicted by the Lockhart-Martinelli correlation with liquid-to-vapor velocity ratios of 0.0, 0.5, and 1.0 and by the Koestel, Gutstein, and Wainwright fog-flow model with a liquid-to-vapor velocity ratio of 1.0 to the measured local pressures. From reference 13, measured

mercury static pressures are shown in figures 3(a), (b), and (c) along with some of the predicted static-pressure profiles used in this report for condensing lengths of 10, 20, and 34 inches, respectively. The predicted static-pressure profile for a liquid-to-vapor velocity ratio of 0.0 was not used in this analysis and is not shown in figure 3, because, in general, it did not agree well with the measured static pressures.

RESULTS AND DISCUSSION

The experimental conditions are presented in table II. The mercury vapor quality leaving the boiler for steady-flow conditions was defined as the ratio of the mercury vapor flow rate leaving the boiler to the liquid flow rate entering the boiler. Because this experimental ratio varied from 0.90 to 1.10, the quality at the inlet of the test section was assumed to be 100 percent for all conditions.

NaK Film Heat-Transfer Coefficient

The NaK Nusselt numbers, evaluated from the experimental NaK film heat-transfer coefficients for test section 1 are presented in figure 4 as a function of the NaK Peclet number. The NaK film heat-transfer coefficients were obtained only at 23.5 and 39.5 inches from the mercury heat-transfer inlet, because the tube-wall thermocouples were inoperative at 7.5, 15.5, and 31.5 inches from the mercury heat-transfer inlet. The range of NaK Peclet number for test section 1 varied from 65 to 127. Also shown in figure 4 is the Nusselt number evaluated for test section 1 by the method proposed in reference 7, in which Dwyer indicates that heat is transferred by molecular conduction for liquid metals flowing in concentric annuli at Peclet numbers below 300. The equation recommended in reference 7 to evaluate the Nusselt number is

$$Nu = 4.92 + 0.686\,y \tag{1}$$

where y is the ratio of outer- to inner-annulus radii. The Nusselt number evaluated from equation (1) was 5.9, resulting in a NaK film heat-transfer coefficient of 4280 Btu/(hr)(sq ft)(^{o}F).

The experimental NaK film heat-transfer coefficients varied from 2530 to 6750 Btu per hour per square foot per ^{o}F (Btu/(hr)(sq ft)(^{o}F)). The resulting NaK Nusselt numbers obtained from these film heat-transfer coefficients varied from 3.5 to 9.3. The arithmetic average of all NaK Nusselt numbers was 5.8, which agreed well with the 5.9 value obtained from equation (1).

Overall Condensing Heat-Transfer Coefficient

The axial temperature profiles of both the mercury and NaK were used to evaluate the overall condensing heat-transfer coefficient for test section 2. Mercury saturation-temperature profiles obtained from the static-pressure profiles were used to evaluate the overall condensing heat-transfer coefficient, since saturation conditions or only slight vapor superheat (less than 5° F) existed at the test-section inlet.

Typical NaK stream and mercury saturation-temperature profiles used to evaluate the overall condensing heat-transfer coefficient are presented in figure 5 for a range of condensing lengths. Two mercury saturation-temperature profiles are shown for each condensing length: (1) the case in which the mercury static pressure and thus saturation temperature were assumed constant and (2) the case in which the saturation temperature was obtained from the calculated mercury-pressure profile with the use of the Lockhart-Martinelli correlation and a liquid-to-vapor velocity ratio of 0.5. The second case was arbitrarily chosen to show the difference between a temperature profile assumed constant and the calculated profile.

A complete comparison of all mercury saturation-temperature profiles acquired from the various static-pressure-profile predictions is presented in figure 6 for the maximum condensing length studied. At this maximum condensing length of 34 inches, the saturation temperatures obtained from the varying static-pressure profiles deviated the greatest amount from the constant-saturation-temperature assumption. Since these temperature deviations are substantial, this figure shows the necessity of considering the varying temperature profile of the condensing fluid when evaluating the overall condensing heat-transfer coefficient by equation (B6). The effect of the temperature difference between the mercury and the NaK on the magnitude of the overall condensing heat-transfer coefficient U is discussed subsequently.

Typical plots of $\int U\, dA_i$ against $\int dA_i$ are presented in figure 7. The plots were obtained by using the temperature profiles presented in figure 5. The slopes of the plots in figure 7 are the overall condensing heat-transfer coefficients U. The values of $\int U\, dA_i$ plotted as a function of $\int dA_i$, obtained for constant-mercury-temperature profiles, tended to deviate slightly from a straight line for the longer condensing lengths. For all condensing lengths, however, the curves of $\int U\, dA_i$ as a function of $\int dA_i$ for both the constant and the varying temperature profiles were approximated by straight lines.

There is no significant difference between the mercury saturation-temperature profiles for condensing lengths less than 15 inches (fig. 5(a)). Consequently, there is no significant difference between the values of $\int U\, dA_i$ for condensing lengths less than 15 inches (fig. 7(a)). As the condensing length was increased beyond 15 inches, however, a significant difference between the assumed constant-temperature profiles

and the varying-temperature profiles progressively increased (figs. 5(b) and (c)). The values of $U\,dA_i$ for both temperature profiles therefore deviate more as the condening length increases (figs. 7(b) and (c)). Furthermore, it is apparent from figure 7 that the local overall heat-transfer coefficient was constant along the condensing length and therefore had the same value as the overall condensing heat-transfer coefficient. The overall condensing heat-transfer coefficients were larger when the varying-temperature profiles were employed because the temperature differences between the mercury saturation temperature and the NaK stream temperature were smaller.

The overall condensing heat-transfer coefficients obtained from test section 2 data are presented for a constant mercury saturation temperature determined by the inlet static pressure (fig. 8(a)), a saturation-temperature profile acquired from the straight lines connecting the measured static pressures (fig. 8(b)), the saturation temperatures obtained from the static-pressure prediction of the Lockhart-Martinelli correlation (ref. 11) with $V_l = V_g/2$ (fig. 8(c)), the saturation temperatures obtained from the static-pressure prediction of the Lockhart-Martinelli correlation with $V_l = V_g$ (fig. 8(d)), and the saturation temperatures determined from the static-pressure predictions of the Koestel, Gutstein, and Wainwright, fog-flow correlation (ref. 12) with $V_l = V_g$ (fig. 8(e)).

When the constant mercury pressure (constant-temperature profile) was assumed, the overall condensing heat-transfer coefficient varied from 1650 to 3420 Btu/(hr)(sq ft)($^{\circ}$F) (fig. 8(a)). The coefficient decreased significantly as the condensing length increased beyond 15 inches. In figure 8(b), the overall condensing heat-transfer coefficient varied from 2500 to 3230 Btu/(hr)(sq ft)($^{\circ}$F) when the mercury temperature was determined by the method in which the measured pressures were connected with straight lines. In this case, there is no apparent tendancy for the coefficient to decrease with an increase of condensing length.

The overall condensing heat-transfer coefficient values obtained when the correlations of Lockhart and Martinelli and of Koestel, Gutstein, and Wainwright were employed to calculate the mercury-pressure variation are presented in figure 8(c) to (e). Compare these three figures with figure 8(b). (The values presented in fig. 8(b) were obtained when the measured pressures were connected with straight lines). The overall condensing heat-transfer coefficient values obtained when correlations were employed are generally 5 to 10 percent higher than the values obtained when the measured pressures were connected with straight lines. Except for condensing lengths less than about 15 inches, the mercury pressure obtained when the correlations were employed were generally lower in the last 25 percent of the condensing length than the pressures obtained by connecting the measured pressures with straight lines. The average values of overall condensing heat-transfer coefficients in figures 8(b) to (e) ranged from 2920 to 3200 Btu/(hr)(sq ft)($^{\circ}$F).

The different values of overall condensing heat-transfer coefficient at the longer condensing lengths (compare fig. 8(a) with figs. 8(b) to (e)) can be explained by referring

to the mercury-temperature profiles presented in figure 6. The NaK temperature profile was the same for all cases. For condensing lengths less than 15 inches, the temperature difference between the mercury and the NaK for each case was not significantly different. At the longer condensing lengths, the temperature difference between the mercury and the NaK was smaller when the mercury temperature was obtained from (1) the calculated mercury-pressure profiles and (2) the mercury-pressure profiles obtained by connecting the measured pressures with straight lines. Therefore, at the longer condensing lengths, the overall condensing heat-transfer coefficient values obtained for the varying mercury pressure and temperature were larger than the values obtained for a constant pressure and temperature.

Relative Magnitude of Mercury-Side, Tube Wall, and NaK-Side Thermal Conductance

Although instrumentation limitations on test section 2 precluded direct measurement of the constituents of the overall heat-transfer coefficient, the relative controlling influence of each can be ascertained from the expression for overall thermal conductance,

$$UA_i = \frac{1}{\frac{1}{h_{Hg}A_i} + \frac{\ln\left(\frac{r_o}{r_i}\right)}{2\pi k_w L} + \frac{1}{h_{NaK}A_o}} \tag{2}$$

Inasmuch as the unknown quantities in this expression are the mercury-side coefficient h_{Hg} and the NaK-side coefficient h_{NaK} the relative magnitudes can be defined by plotting the mercury heat-transfer coefficient as a function of the overall heat-transfer coefficient for fixed values of NaK-side coefficient as shown in figure 9. The averages of the overall coefficient U presented in figures 8(b) to (e) ranged between 2920 and 3200 Btu/(hr)(sq ft)(^{o}F). Furthermore the NaK-side Nusselt number predicted by equation (1) at the midpoint of test section 2 was 5.96, which corresponds to a NaK film coefficient of 5170 Btu/(hr)(sq ft)(^{o}F). Thus the region of intersection of the predicted NaK-side coefficient curve with the band of average overall heat-transfer coefficient indicates mercury-side heat-transfer coefficients an order of magnitude greater than the NaK-side coefficients. The additional curves included in figure 9 illustrate that even though the NaK-side coefficient was substantially greater than the predicted value (e.g., 8000 Btu/(hr)(sq ft)(^{o}F)), the coolant side would still be controlling.

An examination of the relative magnitudes of the NaK-side and tube wall conductances

at the midpoint of test section 2, indicated that neither component was predominantly controlling. The tube wall thermal conductance was 42.5 Btu/(hr)(^{O}F) while the NaK-side conductance was 45.1 Btu/(hr)(^{O}F).

SUMMARY OF RESULTS

The results of an experimental heat-transfer investigation of mercury condensing in horizontal tubes cooled by sodium-potassium (NaK) are summarized as follows:

1. The equation proposed by Dwyer for calculating the Nusselt number for liquid metals flowing in concentric annuli at Peclet numbers below 300 agreed with the average value of the experimentally determined Nusselt numbers from test section 1. The experimental Nusselt numbers ranged between 3.5 to 9.3 and had an average value of 5.8, while the Nusselt number calculated for test section 1 from Dwyer's proposed equation was 5.9.

2. When the mercury saturation temperature was assumed constant for test section 2, the overall condensing heat-transfer coefficient decreased with an increase of condensing length. The overall condensing heat-transfer coefficient decreased from 3420 to 1650 Btu/(hr)(sq ft)(^{O}F) as a function of condensing length. A more accurate evaluation of the overall condensing heat-transfer coefficient for test section 2 was obtained when the mercury saturation temperature variation along the axial length was taken into account. The overall condensing heat-transfer coefficient then became independent of condensing length; average values varied from 2920 to 3200 Btu/(hr)(sq ft)(^{O}F).

3. The mercury-condensing heat-transfer coefficient for test section 2 was concluded to be signficiantly larger than the NaK film heat-transfer coefficient. The tube wall and the predicted NaK-side conductances controlled the heat transfer about equally.

Lewis Research Center,
National Aeronautics and Space Administration,
Cleveland, Ohio, January 31, 1967,
701-04-00-02-22.

APPENDIX A

SYMBOLS

A_i	tube inside surface area
A_o	tube outside surface area
c_p	specific heat of sodium-potassium mixture
D_h	hydraulic diameter (twice annular height)
D_i	inside diameter of mercury tube
h	heat-transfer coefficient
k	thermal conductivity
L	length
l_c	condensing length
Nu	Nusselt number
P	pressure
Pe	Peclet number
Q	heat-transfer rate
r	radius to thermocouple in wall
r_i	inside radius of tube
r_o	outside radius of tube
T	temperature
U	overall condensing heat-transfer coefficient
V	velocity
W	flow rate
x	quality
y	ratio of outer to inner annulus radii
ρ	density

Subscripts:

g	mercury vapor
Hg	mercury
in	inlet
l	liquid mercury
NaK	sodium-potassium
out	outlet
s	static
w	wall
1	any section along tube
2	section 1-in. downstream in direction of mercury flow from section 1

APPENDIX B

DATA REDUCTION AND DERIVATION OF EQUATIONS

Assumptions

The following assumptions were made in reducing the experimental data:

(1) Only radial heat flow

(2) No heat loss to surroundings

(3) NaK bulk temperature profiles represented by faired NaK stream temperature profiles

NaK Film Heat-Transfer Coefficient

The NaK film heat-transfer coefficient was obtained from test section 1 data. The rate of heat transferred from the wall where the thermocouple was located to the NaK flowing in the annulus can be expressed as

$$Q = \frac{T_w - T_{NaK}}{\frac{1}{h_{NaK} A_o} + \frac{\ln\left(\frac{r_o}{r}\right)}{2\pi k_w L}} \tag{B1}$$

Solving for the NaK film heat-transfer coefficient yields

$$h_{NaK} = \frac{1}{\frac{T_w - T_{NaK}}{\frac{Q}{A_o}} - \frac{r_o \ln\left(\frac{r_o}{r}\right)}{k_w}} \tag{B2}$$

The local heat flux Q/A_o was evaluated by the equation,

$$\frac{Q}{A_o} = \frac{W_{NaK} c_p \Delta T_{NaK}}{2\pi r_o \Delta L} \tag{B3}$$

The NaK temperatures were obtained from the temperature profile faired through the averages of the measured NaK stream temperatures. The thermal conductivity for the nicrobrazing material LM 4777 was assumed constant (11 Btu/(hr)(ft)(^{o}F)) for the range of temperature encountered.

Overall Condensing Heat-Transfer Coefficient

Writing a heat-balance equation for an element along the condensing length (fig. 10) yields

$$U\pi D_i \, dL(T_{Hg} - T_{NaK}) = -W_{NaK}c_p \, dT_{NaK} \tag{B4}$$

Rearranging equation (B4) and then adding and subtracting dT_{Hg} to the numerator of the right side yields

$$U\pi D_i \, dL = W_{NaK}c_p \frac{dT_{Hg} - dT_{NaK} - dT_{Hg}}{T_{Hg} - T_{NaK}} \tag{B5}$$

Separating the right side of equation (B5) into two terms and then integrating yields

$$\int_{L_1}^{L_2} U\pi D_i \, dL = W_{NaK}c_p \left[\ln \frac{\left(T_{Hg} - T_{NaK}\right)_{L_2}}{\left(T_{Hg} - T_{NaK}\right)_{L_1}} - \int_{L_1}^{L_2} \frac{\frac{dT_{Hg}}{dL}}{T_{Hg} - T_{NaK}} dL \right] \tag{B6}$$

The term $\int U \, dA_i$ was plotted as a function of $\int dA_i$. The slope of the curve obtained then was the value of the overall condensing heat-transfer coefficient U.

REFERENCES

1. Baker, R. A.; and Sosonske, Alexander: Heat Transfer in Sodium-Potassium Alloy. Nucl. Sci. Eng., vol. 13, no. 3, July 1962, pp. 283-288.

2. Duchatelle, L.; and Vautrey, L.: Determination des coefficients de convection d'un alliage NaK en ecoulement turbulent entre plaques planes parellels. Int. J. Heat Mass Transfer, vol. 7, no. 9, Sept. 1964, pp. 1017-1031.

3. Sawochka, S. G.; and Schleef, D. J.: Liquid Heat-Transfer Coefficients for Potassium During Vertical Upflow Inside a Tube. Paper no. 64 WA/HT-19, ASME, Nov. 29-Dec. 4, 1964.

4. Sowatchka, S. C.: Thermal and Fluid Dynamic Performance of Potassium During Condensing Inside a Tube. Paper Presented at the AIAA Rankine Cycle Space Power System Specialist Conference, NASA Lewis Research Center, Oct. 26-28, 1965.

5. Lyon, Richard N.: Liquid Metal Heat-Transfer Coefficients. Chem. Eng. Progr., vol. 47, no. 2, Feb. 1951, pp. 75-79.

6. Dwyer, O. E.; and Tu, P. S.: Unilateral Heat Transfer to Liquid Metals Flowing in Annuli. Nucl. Sci. Eng., vol. 15, no. 1, Jan. 1962, pp. 58-68.

7. Dwyer, O. E.: Eddy Transport in Liquid-Metal Heat Transfer. AIChE J., vol. 9, no. 2, Mar. 1963, pp. 261-268.

8. Dwyer, O. E.; and Lyon, R. N.: Liquid-Metal Heat Transfer. Reactor Engineering and Equipment. Vol. 8 of the Proceedings of the Third International Conference on the Peaceful Uses of Atomic Energy, United Nations, 1965, pp. 182-189.

9. Kunz, H. R.: Analytical Study of Liquid Metal Condensing Inside Tubes. Rep. No. PWA-2530 (NASA CR-54352), Pratt & Whitney Aircraft, Jan. 1965.

10. Ross, D. P.: Thermodynamic Properties of Mercury. Rep. No. TM-777, Thompson Ramo Wooldridge, Inc., June 1957.

11. Lockhart, R. W.; and Martinelli, R. C.: Proposed Correlation of Data for Isothermal Two-Phase, Two-Component Flow In Pipes. Chem. Eng. Progr. vol. 45, no. 1, Jan. 1949, pp. 39-48.

12. Koestel, Alfred; Gutstein, Martin U.; and Wainwright, Robert T.: Study of Wetting and Nonwetting Mercury Condensing Pressure Drop. NASA TN D-2514, 1964.

13. Vernon, Richard W.; Lottig, Roy A.; and Kenney, William D.: Experimental Investigation of the Pressure Characteristics of Nonwetting, Condensing Flow of Mercury in a Sodium-Potassium Cooled, Tapered Tube. NASA TN D-3691, 1966.

TABLE I. - TRANSDUCER LOCATION AND CALIBRATION RANGE

Pressure transducer	Description	Calibration range, psi
[a]PT_0	Pressure between mercury inlet flange and NaK outlet	[b]0 to 10
PT_2	Pressure drop across orifice	[b]0 to 80
PT_3	Boiler inlet pressure	[c]0 to 200
[d]PT_4	Pressure between mercury inlet flange and NaK outlet	[c]0 to 32
[d]PT_5	Pressure at mercury outlet flange	[c]0 to 32
PT_6	Venturi inlet pressure	[c]0 to 32
PT_7	Venturi pressure drop	[b]0 to 5
PT_8	NaK outlet pressure	[c]0 to 50
PT_9	NaK inlet pressure	[c]0 to 50
[a]PT_{12}	Pressure 12 in. from mercury heat transfer inlet	[b]0 to ±5
PT_{13}	Reference manifold pressure	[c]0 to 24
[a]PT_{15}	Receiver pressure	[c]0 to 32
[a]PT_{25}	Pressure 25 in. from mercury heat transfer inlet	[b]0 to ±5
[a]PT_{38}	Pressure 38 in. from mercury heat transfer inlet	[b]0 to ±5
[a]PT_{51}	Pressure at mercury outlet flange	[b]0 to 10

[a]Used only on test section 2.
[b]Differential transducer.
[c]Absolute transducer.
[d]Used only on test section 1.

TABLE II. - EXPERIMENTAL DATA

(a) Test section 1

Run	Inlet mercury flow rate, W_{Hg}, lb/hr	NaK flow, rate W_{NaK}, lb/hr	Condensing length, l_c, in.	NaK inlet temperature, $T_{NaK,in}$, ^{o}F	NaK outlet temperature, $T_{NaK,out}$, ^{o}F	Mercury tube inlet temperature, $T_{Hg,in}$, ^{o}F	Calculated mercury inlet quality, x
1	150	726	27	510	647	697	1.05
2	149	677	27	510	647	697	1.04
3	147	691	27	512	645	699	1.03
4	149	701	28	512	649	699	1.05
5	147	652	28	510	647	699	1.04
6	129	407	31	446	656	693	.91
7	126	422	31	446	654	693	.89
8	184	546	34	444	641	695	1.07
9	187	546	34	444	641	695	1.09
10	188	546	34	444	641	695	1.10
11	189	546	34	446	643	695	1.10
12	181	443	35	398	642	695	1.06
13	182	443	35	402	643	697	1.07
14	182	443	36	402	645	697	1.07
15	185	443	36	399	645	697	1.07
16	186	443	36	401	645	697	1.08
17	183	443	36	402	647	699	1.06
18	188	443	36	402	645	697	1.10
19	185	443	36	402	647	697	1.08
20	187	443	36	402	647	697	1.09
21	183	443	37	403	643	697	1.07
22	186	443	37	402	647	699	1.08
23	190	443	37	402	647	699	1.11
24	131	485	37	502	657	693	1.04
25	134	485	37	500	657	693	1.08
26	134	485	38	500	655	693	1.08
27	135	485	38	496	656	693	1.07
28	134	485	39	499	656	693	1.09
29	134	485	39	500	657	693	1.07
30	133	485	39	499	656	693	1.06
31	169	425	40	444	660	677	.98
32	167	503	41	446	660	675	.97
33	166	439	41	446	660	675	.95
34	155	376	42	450	695	706	.90
35	114	659	42	549	660	690	.98

(b) Test section 2

Run	Inlet mercury flow rate, W_{Hg}, lb/hr	NaK flow rate, W_{NaK}, lb/hr	Condensing length, l_c, in.	NaK inlet temperature, $T_{NaK,in}$, ^{o}F	NaK outlet temperature, $T_{NaK,out}$, ^{o}F	Mercury tube inlet temperature, $T_{Hg,in}$, ^{o}F	Calculated mercury inlet quality, x	Mercury inlet static pressure, $P_{s,in}$, psia	Mercury static pressure at 12 in., $P_{s,12}$, psia	Mercury static pressure at 25 in., $P_{s,25}$, psia	Mercury static pressure at 38 in., $P_{s,38}$, psia	Mercury outlet static pressure, $P_{s,out}$, psia
6	161	514	9	496	686	702	1.05	19.55	19.86	19.92	19.56	19.74
7	149	516	10	497	687	698	.97	18.93	19.70	19.82	19.30	19.50
8	149	517	10	497	682	696	.97	19.29	19.10	19.12	18.58	18.82
9	161	515	10	496	682	696	1.05	18.45	18.78	18.80	18.61	18.59
10	153	515	10	495	685	696	1.03	18.92	19.28	19.22	19.03	19.16
11	156	514	11	504	686	698	1.02	18.73	19.60	19.88	19.30	19.55
12	154	516	11	497	687	696	1.00	18.34	19.20	19.37	18.80	19.00
13	149	515	11	498	683	691	.98	17.34	18.20	18.30	17.72	17.98
14	161	514	12	497	682	689	1.06	17.30	17.60	17.68	17.50	17.54
15	154	517	13	498	686	692	1.00	17.84	18.60	18.74	18.27	18.49
16	160	516	13	497	684	691	1.04	17.77	17.98	18.17	17.82	17.94
17	159	516	14	502	683	688	1.03	17.16	17.23	17.62	17.30	17.40
18	155	515	14	496	688	690	1.01	17.76	18.10	18.11	18.07	18.05
19	155	515	14	502	687	690	1.01	17.70	17.92	18.19	18.09	18.15
20	149	515	15	497	682	690	1.02	17.24	17.69	18.30	-----	17.84
21	156	515	15	497	683	687	1.02	17.00	16.79	17.42	17.03	17.20
22	160	516	15	496	684	687	1.04	16.90	16.80	17.40	17.26	17.19
23	157	515	15	497	684	688	1.02	17.48	17.33	17.80	17.79	17.79
24	153	515	18	498	684	687	1.00	16.97	16.83	18.17	17.62	17.66
25	152	517	19	497	687	689	1.00	17.08	16.66	18.10	17.61	17.78
26	152	517	20	498	683	686	.98	16.59	15.99	17.59	-----	17.15
27	161	516	20	503	682	684	1.05	16.63	15.68	16.90	16.87	17.04
28	162	513	20	503	687	688	1.01	17.38	16.46	17.63	17.74	17.84
29	158	515	20	502	684	687	1.03	16.91	15.90	16.99	17.24	17.33
30	153	515	21	497	686	688	1.00	17.00	16.40	18.04	17.52	17.70
31	158	513	23	503	685	686	1.03	16.82	15.72	16.76	17.01	17.13
32	153	517	24	499	684	687	1.00	16.71	15.94	17.12	17.24	17.40
33	161	515	24	502	685	686	1.04	16.70	15.52	16.49	16.95	16.90
34	158	513	24	502	685	687	1.02	17.11	16.00	16.95	17.34	17.33
35	150	517	25	499	686	687	.98	16.99	16.25	17.30	17.50	17.54
36	163	516	27	496	686	688	1.06	17.09	15.86	16.12	17.05	17.24
37	163	515	27	498	685	686	1.06	16.64	15.47	16.11	16.69	16.73
38	158	515	29	500	682	682	1.03	16.12	14.93	14.02	15.63	15.91
39	161	515	29	497	686	686	1.05	17.08	15.80	14.74	16.57	16.92
40	159	513	29	500	684	686	1.04	16.86	15.62	14.44	16.49	17.02
41	152	518	30	495	686	686	.99	16.56	15.75	14.20	16.98	17.15
42	159	516	32	500	685	686	1.04	17.13	15.88	13.43	16.26	16.45
43	158	515	34	498	685	686	1.03	16.92	15.62	12.81	16.92	16.88

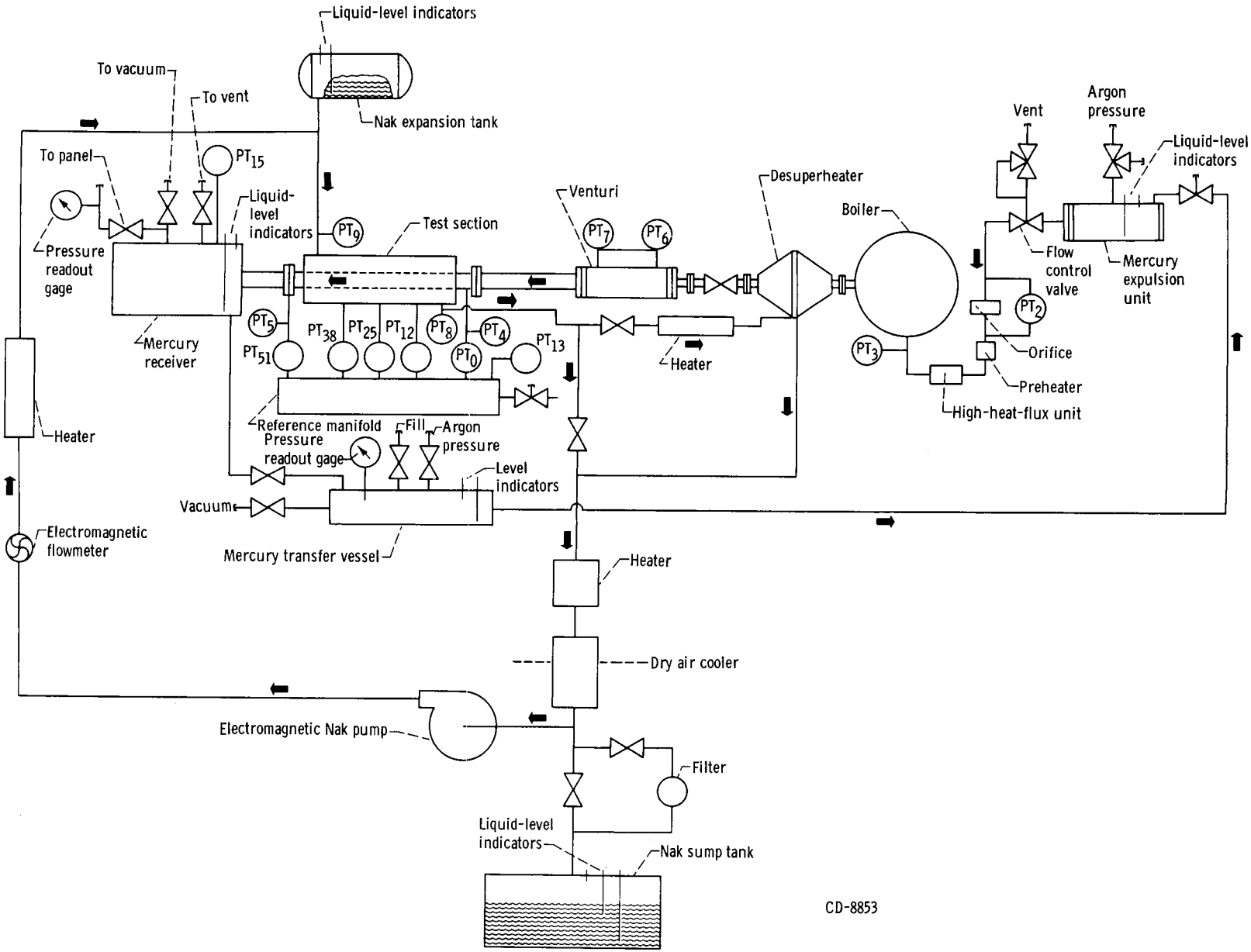

Figure 1. - Mercury and sodium-potassium test facility.

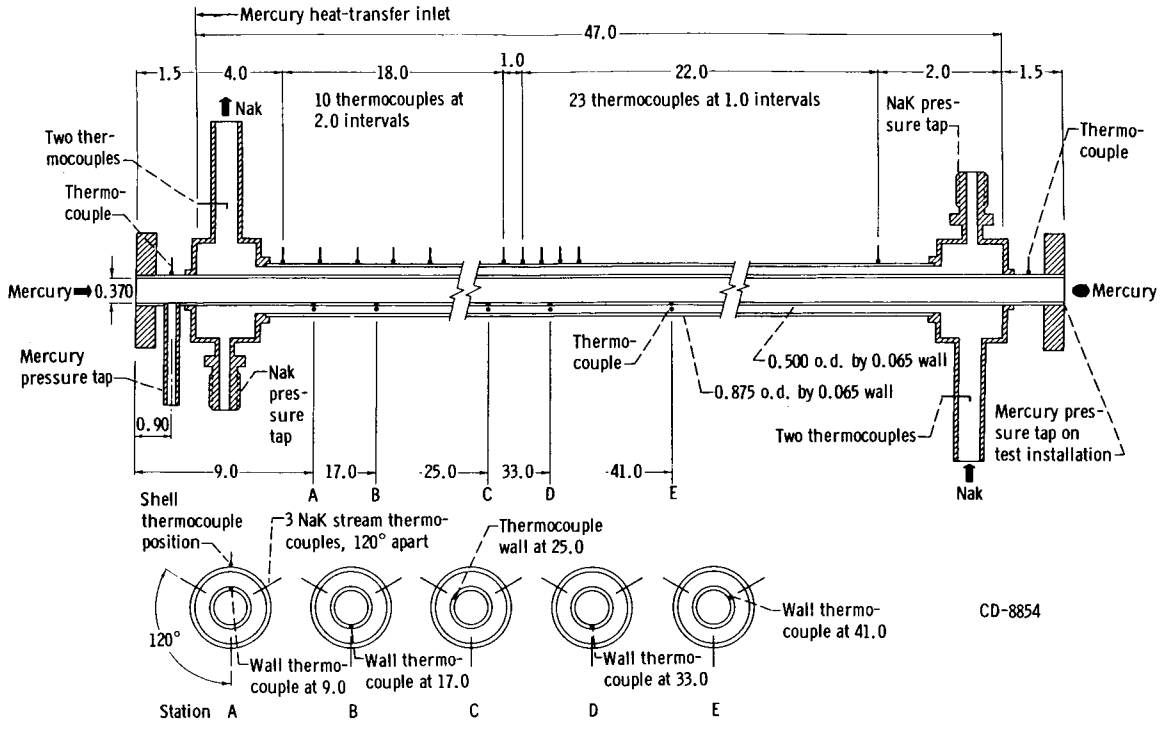

(a) Test section 1 (constant diameter).

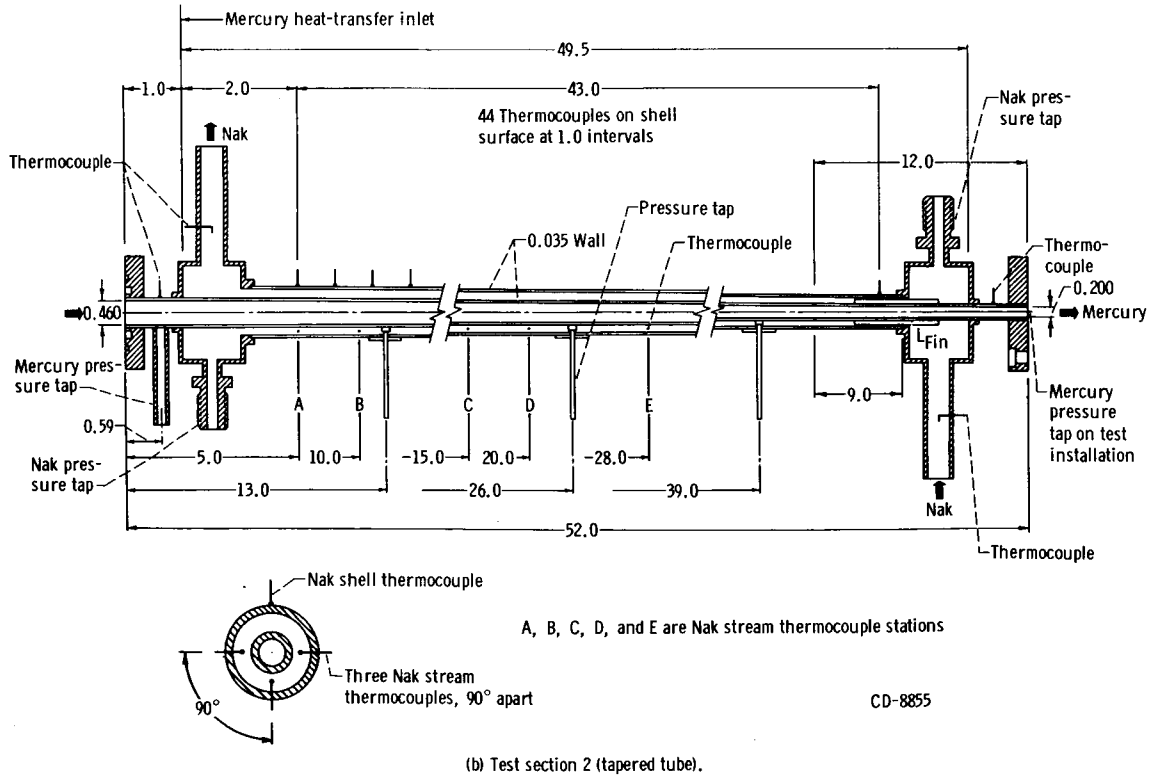

(b) Test section 2 (tapered tube).

Figure 2. - Experimental test sections. (All dimensions in inches except where otherwise noted.)

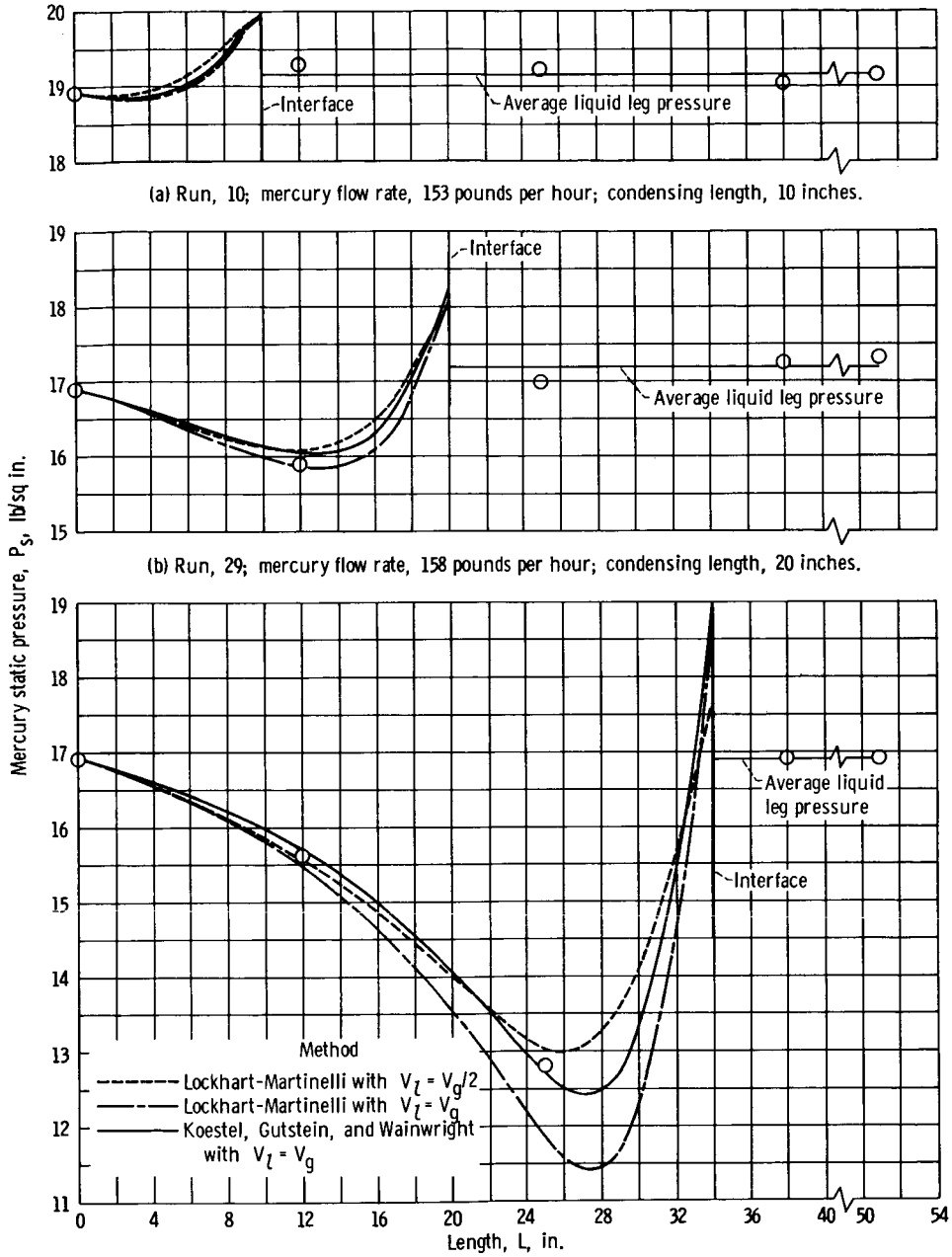

(a) Run, 10; mercury flow rate, 153 pounds per hour; condensing length, 10 inches.

(b) Run, 29; mercury flow rate, 158 pounds per hour; condensing length, 20 inches.

(c) Run, 43; mercury flow rate, 158 pounds per hour; condensing length, 34 inches.

Figure 3. - Static-pressure predictions as function of length for test section 2. NaK flow rate, 515 pounds per hour.

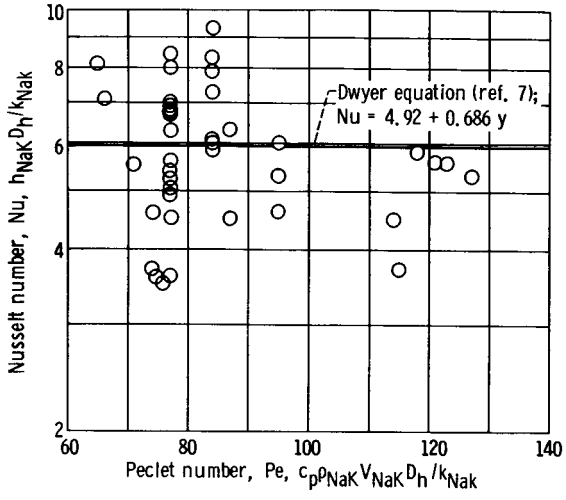

Figure 4. - Variation of Nusselt number with Peclet number for test section 1.

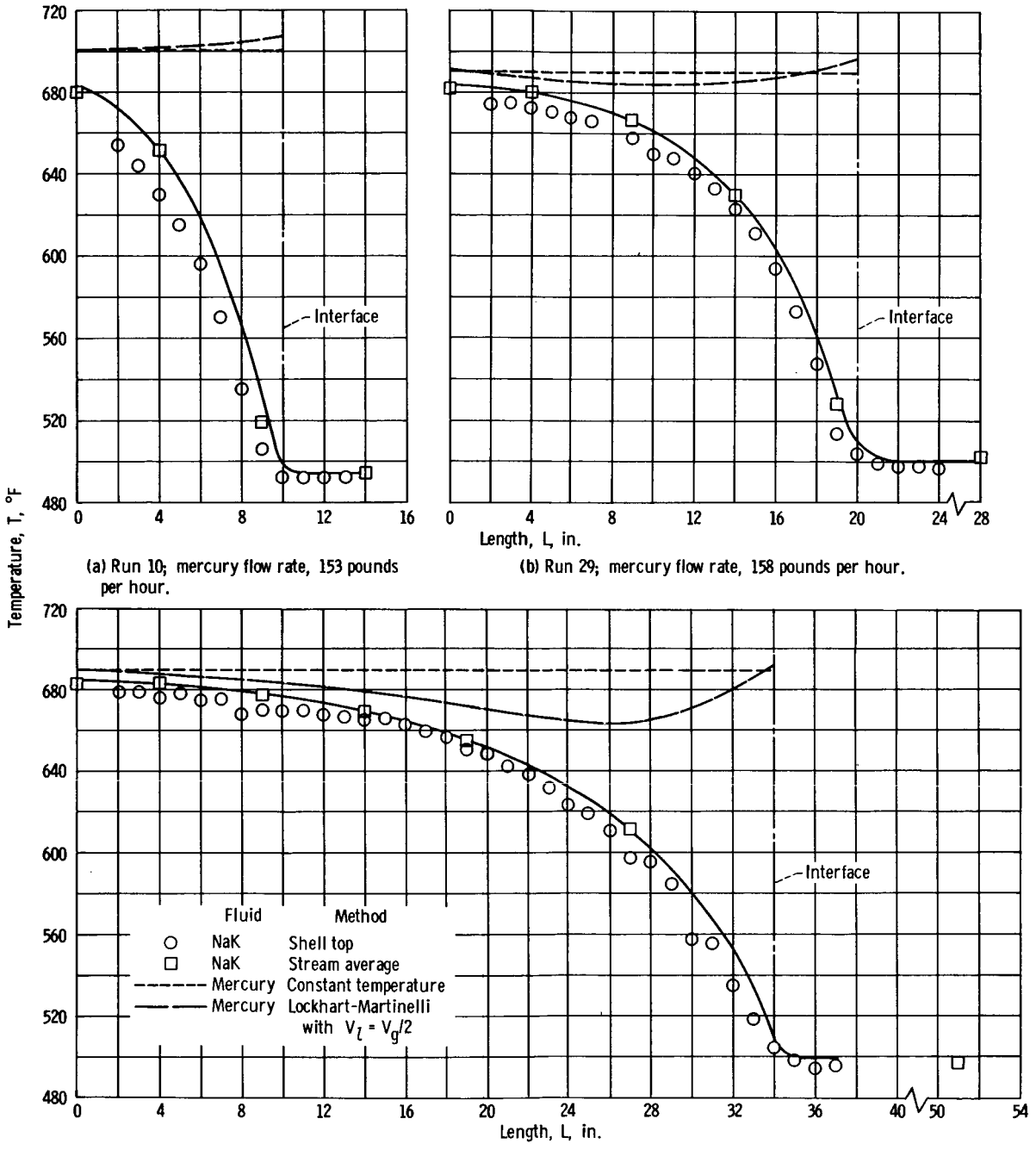

(a) Run 10; mercury flow rate, 153 pounds per hour.

(b) Run 29; mercury flow rate, 158 pounds per hour.

(c) Run 43; mercury flow rate, 158 pounds per hour.

Figure 5. - Temperature profiles of NaK and condensing mercury for test section 2. NaK flow rate, 515 pounds per hour.

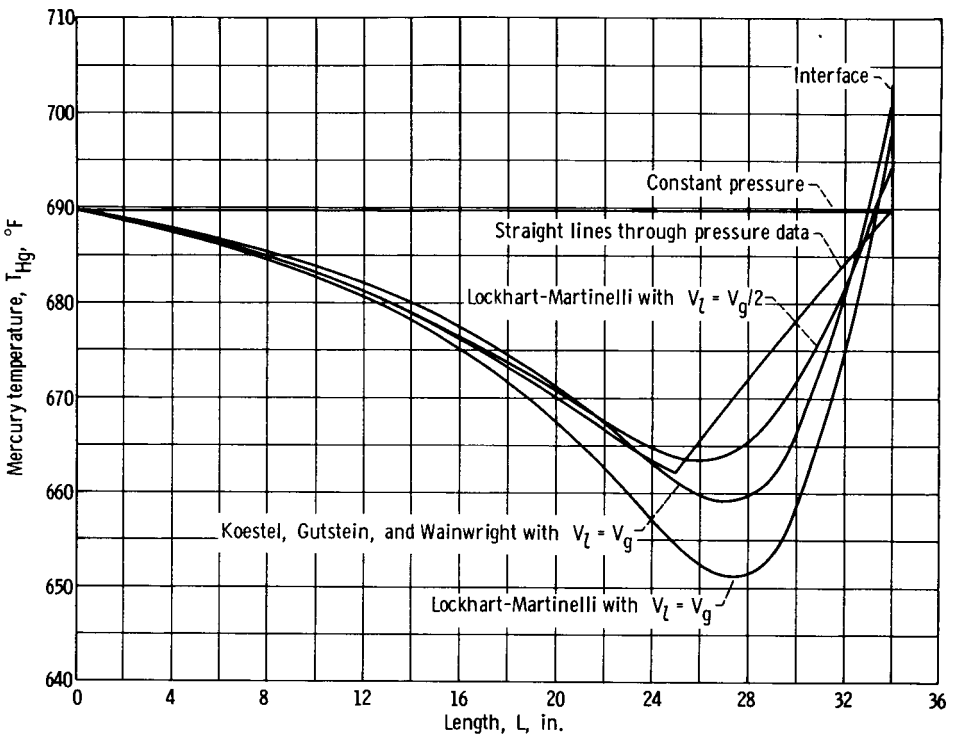

Figure 6. - Mercury saturation-temperature profiles obtained from various methods of estimating mercury static-pressure profiles along condensing length for test section 2. Run 43; mercury flow rate, 158 pounds per hour; NaK flow rate, 515 pounds per hour.

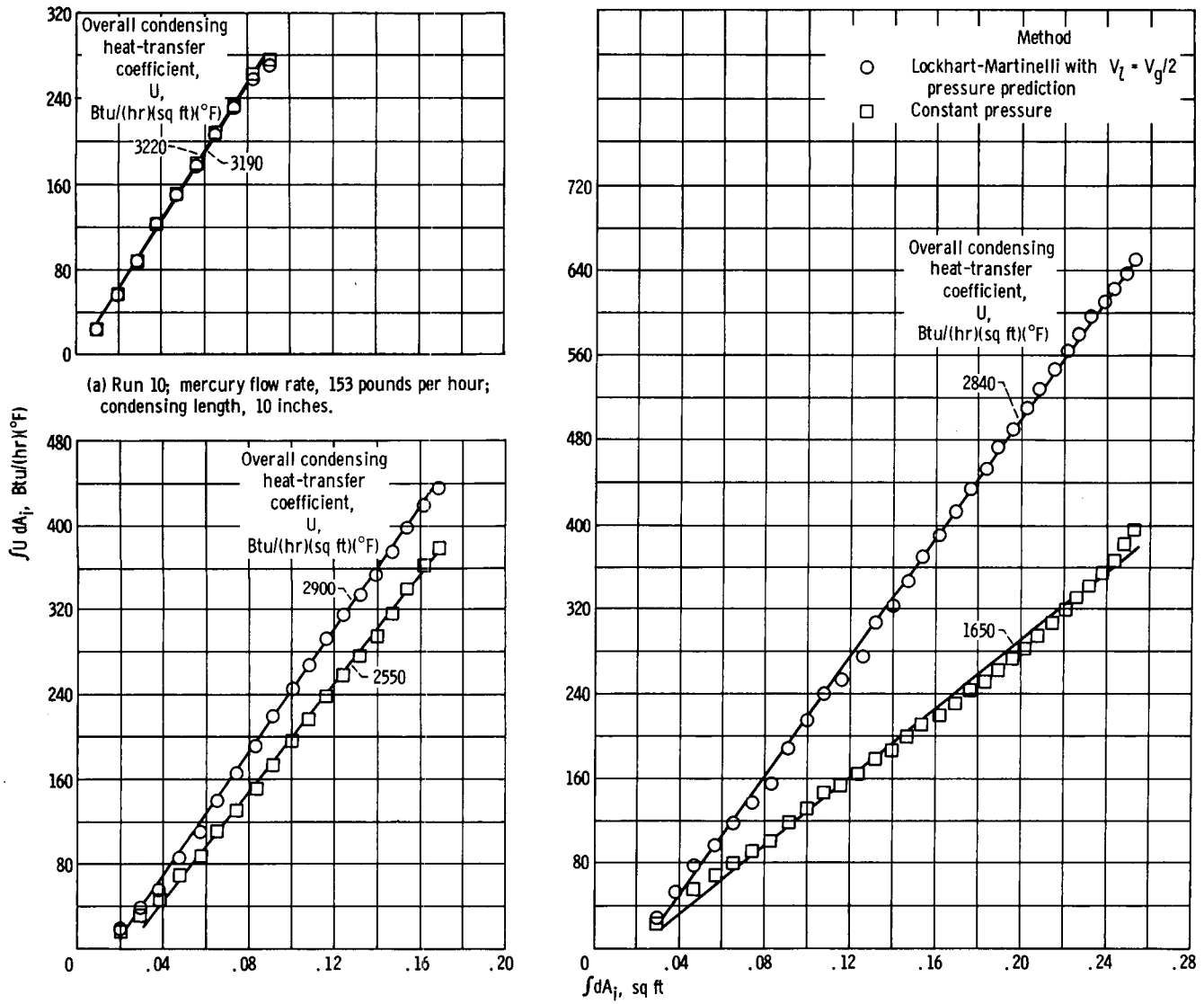

(a) Run 10; mercury flow rate, 153 pounds per hour; condensing length, 10 inches.

(b) Run 29; mercury flow rate, 158 pounds per hour; condensing length, 20 inches.

(c) Run 43; mercury flow rate, 158 pounds per hour; condensing length, 34 inches.

Figure 7. - Variation of $\int U\, dA_i$ with $\int dA_i$ for test section 2. NaK flow rate, 515 pounds per hour.

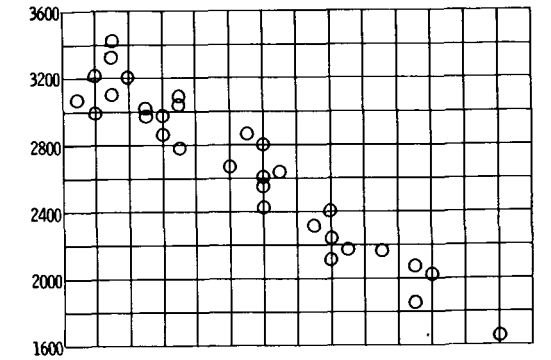

(a) Constant static pressure.

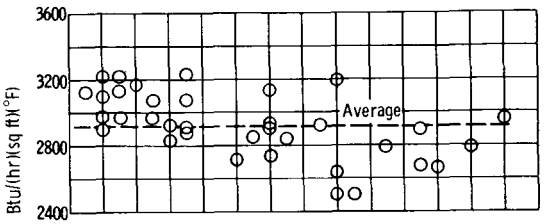

(b) Static pressure from straight lines connecting local measured static pressures.

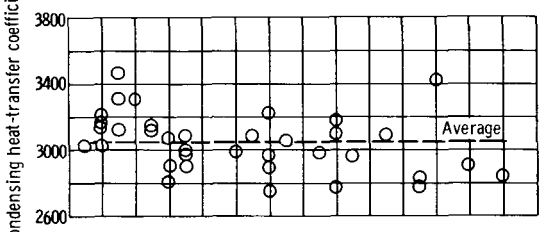

(c) Two-phase static-pressure correlation of Lockhart and Martinelli with liquid-to-vapor velocity ratio of 1/2.

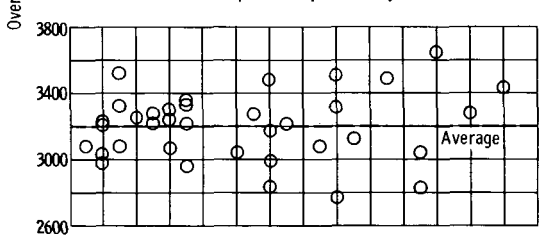

(d) Two-phase static-pressure correlation of Lockhart and Martinelli with liquid-to-vapor velocity ratio of 1.

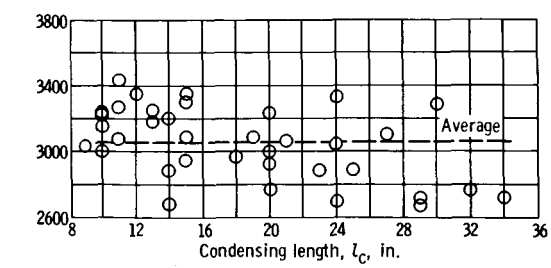

(e) Two-phase static-pressure correlation of Koestel, Gutstein, and Wainwright with liquid-to-vapor velocity ratio of 1.

Figure 8. - Overall condensing heat-transfer coefficient as function of condensing length for test section 2. Mercury flow rate, 155 pounds per hour; NaK flow rate, 515 pounds per hour.

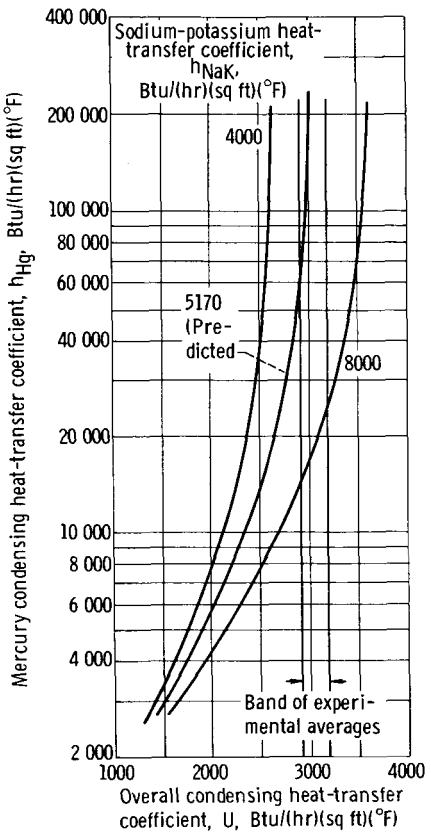

Figure 9. - Mercury-condensing heat-transfer coefficient evaluated at midpoint of tapered length as function of overall condensing heat-transfer coefficient for test section 2.

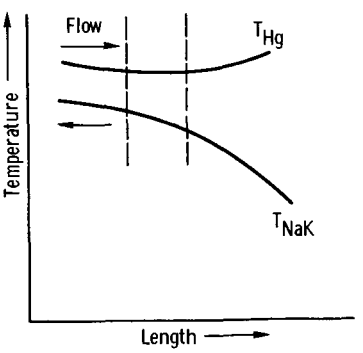

Figure 10. - Element of mercury and NaK temperature profiles.

NASA-Langley, 1967 — 12 E-3608